Collisional m_J mixing and multipole relaxation in 4^2P potassium atoms

P. Skalinski and L. Krause
Department of Physics, University of Windsor, Windsor N9B 3P4 Canada
(Received 18 February 1982)

m_J mixing in $4^2P_{1/2}$ and $4^2P_{3/2}$ potassium atoms as well as atomic multipole relaxation induced in K-K and K-Ar collisions were investigated by methods of atomic fluorescence spectroscopy. K vapor, pure or mixed with Ar, was placed in a kG magnetic field and irradiated with a single Zeeman component of 7665- or 7699-Å resonance radiation, causing the selective excitation of the $^2P_{1/2,-1/2}$ or $^2P_{3/2,-3/2}$ substate. Collisions of the excited atoms with ground-state K or Ar atoms caused m_J mixing which was monitored by analysis of the resulting fluorescent spectrum with a scanning Fabry-Perot interferometer. Intensity measurements on the fluorescent Zeeman components in relation to ground-state atomic densities yielded the following multipole relaxation cross sections $\Lambda_J^{(L)}$: K-K (10^{-12} cm^2): $\Lambda_{1/2}^{(1)}=5.7\pm0.9$, $\Lambda_{3/2}^{(1)}=8.1\pm1.4$, $\Lambda_{3/2}^{(2)}=11.4\pm2.0$, $\Lambda_{3/2}^{(3)}=9.8\pm1.5$; K-Ar ($10^{-16}$ cm^2): $\Lambda_{1/2}^{(1)}=65\pm10$, $\Lambda_{3/2}^{(1)}=175\pm25$, $\Lambda_{3/2}^{(2)}=230\pm35$, $\Lambda_{3/2}^{(3)}=190\pm30$. The $Q_J(m\leftrightarrow m')$ cross sections for m_J mixing were derived from the $\Lambda_J^{(L)}$ as well as the cross sections for multipole decay $\sigma_J^{(L)}=\Lambda_J^{(L)}+\sigma_J^{(0)}$. The experimental results are in good agreement with theoretical calculations.

I. INTRODUCTION

When alkali-metal vapor contained in a fluorescence cell is irradiated with polarized alkali-metal resonance radiation, the atoms become preferentially excited to certain Zeeman sublevels of the resonance states; this results in the creation of a bulk multipole moment in the vapor, which manifests itself in the polarization of the emitted resonance fluorescence. Collisions between the excited alkali-metal atoms and ground-state alkali-metal or other atoms tend to equalize the Zeeman populations and cause relaxation of the atomic multipoles accompanied by the depolarization of the fluorescence. The study of such depolarization or of changes in the populations of the (excited) Zeeman substates in relation to the density of the ground-state atoms inducing the relaxation leads to cross sections for m_J mixing or multipole relaxation.[1] When the fluorescing vapor is placed in a magnetic field strong enough to effectively decouple the nuclear from the electronic moments, the measured cross sections are not perturbed by the "flywheel effect" of the nucleus.[2] Experiments of this kind, employing a modified Zeeman scanning method, yielded cross sections for dipole and quadrupole relaxation (disorientation and disalignment) in $4^2P_{1/2}$ and $4^2P_{3/2}$ potassium atoms induced in collisions with noble gas atoms and in resonant collisions with ground-state potassium atoms.[3–6] To detect octapole relaxation it is necessary to resolve the individual Zeeman components in the fluorescent light. Such spectroscopic resolution of the Zeeman fluorescent spectrum was employed by Gay and Schneider, who determined cross sections for transfers between the 3^2P Zeeman components in sodium and for relaxation of the multipoles induced in collisions with noble gases[7] and with ground-state Na atoms.[8] Most recently, Boggy and Franz measured similar cross sections for collisions of potassium with Ne, Kr, and Xe atoms.[9]

In this investigation, we report the results of an experiment in which we excited selected $4^2P_{1/2}$ or $4^2P_{3/2}$ Zeeman substates in potassium at a magnetic field of about 8 kG and followed transfer of population between the Zeeman sublevels induced in collisions with ground-state K or Ar atoms. The resulting cross sections for Zeeman mixing, multipole relaxation, and collisional decay of the multipoles are compared with previously reported experimental results and with theoretical calculations of Lewis, Wheeler, and Wilson[10] for K-Ar collisions and of Carrington, Stacey, and Cooper[11] for the resonant K-K collisions.

II. THEORETICAL

The method by which light emitted from an rf potassium discharge may be used to selectively

populate Zeeman sublevels of 4^2P potassium resonance states has been described previously.[4] Collisions with atoms of an added buffer gas or with ground-state potassium atoms tend to equalize the Zeeman state populations:

$$\mathrm{K}(4^2P_{1/2,m})+X \leftrightarrow \mathrm{K}(4^2P_{1/2,m'})+X \ , \tag{1}$$

$$\mathrm{K}(4^2P_{3/2,m})+X \leftrightarrow \mathrm{K}(4^2P_{3/2,m'})+X \ , \tag{2}$$

where X is a ground-state atom and m or $m'=3/2$, $1/2$, $-1/2$, $-3/2$. Continuous optical excitation results in a steady state which involves spontaneous decay to the ground state as well as collisional transfers between the Zeeman substates, and which may be represented by the following rate equations:

$$\frac{dN_m}{dt}=-\frac{N_m}{\tau}-N_m\sum_{m'\neq m}Z(m\rightarrow m') + \sum_{m'\neq m}N_{m'}Z(m\leftarrow m')+S_m=0 \ , \tag{3}$$

where Z is the frequency of collisions per excited atom, corresponding to transfer between the optically populated state m and the other states m'. N_m is the population density of the Zeeman substates, S_m is the density of atoms excited per second to state m, and $\tau=2.77\times10^{-8}$ s is the mean lifetime of the 4^2P state.[12] The m_J mixing cross sections may be defined analogously with the gas-kinetic cross section,

$$Z(m\rightarrow m')=NQ(m\rightarrow m')v_r \ , \tag{4}$$

where N is the density of the ground-state collision partners, and v_r is the average relative speed of the colliding atoms. Equations (1)–(3) take no account of collisional $^2P_{1/2}$-$^2P_{3/2}$ fine-structure mixing or quenching to the ground state.

The multipole densities $n^{(L)}$ may be expressed in terms of N_m by means of the following equations yielded by an application of density-matrix formalism in its irreducible tensor representation.[1,13,14]

For the $^2P_{1/2}$ state, the monopole or occupation component ($L=0$) is

$$n^{(0)}_{1/2}=\frac{1}{\sqrt{2}}(N_{1/2}+N_{-1/2}) \ , \tag{5}$$

and the dipole or orientation component ($L=1$) is

$$n^{(1)}_{1/2}=\frac{1}{\sqrt{2}}(N_{1/2}-N_{-1/2}) \ . \tag{6}$$

For the $^2P_{3/2}$ state, the monopole or occupation component ($L=0$) is

$$n^{(0)}_{3/2}=\frac{1}{2}(N_{3/2}+N_{1/2}+N_{-1/2}+N_{-3/2}) \ , \tag{7}$$

the dipole or orientation component ($L=1$) is

$$n^{(1)}_{3/2}=\frac{1}{2\sqrt{5}}(3N_{3/2}+N_{1/2}-N_{-1/2}-3N_{-3/2}) \ , \tag{8}$$

the quadrupole or alignment component ($L=2$) is

$$n^{(2)}_{3/2}=\frac{1}{2}(N_{3/2}-N_{1/2}-N_{-1/2}+N_{-3/2}) \ , \tag{9}$$

and the octapole component ($L=3$) is

$$n^{(3)}_{3/2}=\frac{1}{2\sqrt{5}}(N_{3/2}-3N_{1/2}+3N_{-1/2}-N_{-3/2}) \ . \tag{10}$$

Equations (5)–(10) take no account of nuclear spin and assume the absence of off-diagonal coherence in the $^2P_{3/2}$ state. The dynamic equilibrium involving the populations of the Zeeman substates may also be represented in terms of rate equations involving the multipole moments. Because the collisions are isotropic, each multipole moment relaxes independently:

$$\frac{dn^{(L)}_J}{dt}=s^{(L)}_J-n^{(L)}_J/\tau-\gamma^{(L)}_J n^{(L)}_J=0 \ , \tag{11}$$

where $s^{(L)}_J$ is the $2^{L\text{th}}$ multipole component of the excitation function, which may be expressed in terms of the S_m, and $\gamma^{(L)}_J$ are the multipole relaxation rates. Equation (11) has a solution

$$n^{(L)}_J=\tau s^{(L)}_J/(1+\gamma^{(L)}_J\tau) \ . \tag{12}$$

In the absence of collisional depopulation, $\gamma^{(0)}_J=0$ and $n^{(0)}_J=\tau s^{(0)}_J$. This result together with Eq. (12) yields an expression

$$\tau\gamma^{(L)}_J=(n^{(0)}_J/n^{(L)}_J)(s^{(L)}_J/s^{(0)}_J)-1 \tag{13}$$

from which it is possible to calculate $\gamma^{(L)}_J$ and the cross sections $\Lambda^{(L)}_J$ for collisional relaxation of the multipole moments, since

$$\gamma^{(L)}_J=N\Lambda^{(L)}_J v_r \ . \tag{14}$$

By monitoring the populations of the individual Zeeman substates in relation to the buffer gas pressure and substituting these in Eqs. (6)–(10), it is possible to obtain the $n^{(L)}_J$ densities which, used in conjunction with Eqs. (13) and (14), yield the mul-

tipole relaxation rates $\gamma_J^{(L)}$ and cross sections $\Lambda_J^{(L)}$. The latter are related as follows[4] to the cross sections $Q_J(m \to m')$.

For the $^2P_{1/2}$ state

$$Q_{1/2}(\tfrac{1}{2} \leftrightarrow -\tfrac{1}{2}) = \tfrac{1}{2}\Lambda_{1/2}^{(1)} . \tag{15}$$

For the $^2P_{3/2}$ state

$$Q_{3/2}(\tfrac{1}{2} \leftrightarrow -\tfrac{1}{2}) = \tfrac{1}{20}\Lambda_{3/2}^{(1)} - \tfrac{1}{4}\Lambda_{3/2}^{(2)} + \tfrac{9}{20}\Lambda_{3/2}^{(3)} , \tag{16}$$

$$Q_{3/2}(\tfrac{3}{2} \leftrightarrow \tfrac{1}{2}) = -\tfrac{3}{20}\Lambda_{3/2}^{(1)} + \tfrac{1}{4}\Lambda_{3/2}^{(2)} + \tfrac{3}{20}\Lambda_{3/2}^{(3)} , \tag{17}$$

$$Q_{3/2}(\tfrac{3}{2} \leftrightarrow -\tfrac{1}{2}) = \tfrac{3}{20}\Lambda_{3/2}^{(1)} + \tfrac{1}{4}\Lambda_{3/2}^{(2)} - \tfrac{3}{20}\Lambda_{3/2}^{(3)} , \tag{18}$$

$$Q_{3/2}(\tfrac{3}{2} \leftrightarrow -\tfrac{3}{2} = \tfrac{9}{20}\Lambda_{3/2}^{(1)} - \tfrac{1}{4}\Lambda_{3/2}^{(2)} + \tfrac{1}{20}\Lambda_{3/2}^{(3)} . \tag{19}$$

Because the Zeeman splitting $\ll kT$, there is symmetry in the m_J mixing cross sections:

$$Q(m \leftrightarrow m') = Q(-m \leftrightarrow -m') . \tag{20}$$

It can be seen that, if the populations of the Zeeman sublevels can be determined in relation to the buffer gas density, it is possible to obtain the cross sections for transfer between the individual Zeeman substates as well as for relaxation of all the multipole moments. The populations are derived from the intensities of the Zeeman components of the fluorescent spectrum, bearing in mind that the fluorescence was circularly polarized and was observed in a direction parallel to the magnetic field surrounding the fluorescence cell, and that $A'_\sigma : A_\sigma : A_\pi = 6:2:4$, where A_σ and A_π are the transition probabilities for the decays of the $^2P_{3/2,\pm 1/2}$ substates taking place by emission of $\sigma^\pm$ and π-polarized radiation, respectively, and A'_σ is the corresponding transition probability for the $^2P_{3/2,\pm 3/2}$ substates. Accordingly, while the intensity of the $\sigma^\pm$-polarized fluorescent radiation emitted in the decay of the $^2P_{3/2,\pm 3/2}$ substate is proportional to its population, the $\sigma^\pm$ intensity arising from the $^2P_{3/2,\pm 1/2}$ substate is proportional to $\frac{1}{3}$ its population. In the $^2P_{1/2}$ state, the $\sigma^\pm$ intensity represents $\frac{2}{3}$ population of the $m_J = \pm 1/2$ state.[15]

The connection between the measured intensities of the Zeeman components and the Zeeman mixing cross sections $Q_J(m \to m')$ is provided by Eqs. (3) and (4), while Eqs. (5)–(10) together with (12) and (14) connect the Zeeman intensities with the multipole relaxation cross sections.

According to the generally accepted definition,[1] the total cross sections $\sigma_J^{(L)}$ for the collisional decay of the multipole moments may be represented as

$$\sigma_J^{(L)} = \Lambda_J^{(L)} + \sigma_J^{(0)} , \tag{21}$$

where in this case $\sigma_J^{(0)}$ is the cross section for $J \to J'$ fine-structure mixing.

III. EXPERIMENTAL

The arrangement of the apparatus is shown in Fig. 1. Light from an electrodeless rf lamp,[16] placed together with a totally reflecting prism in a magnetic field of 5.4 kG, was passed through an interference filter, quarter-wave plate and linear polarizer and brought to a focus inside the fluorescence cell containing potassium vapor and located in a constant magnetic field of about 8 kG. (Spectrolab interference filters transmitting the 7665-Å component for the excitation of the $^2P_{3/2}$ state or the 7699-A component for the excitation of the $^2P_{1/2}$ state had a transmission of about 35% and rejection of 0.1%.) The resulting fluorescence, emerging at right angles to the direction of the excitating light beam through a hole in the pole piece of the magnet, was resolved with a scanning Fabry-Perot interferometer and detected with a photomultiplier whose signal was amplified and registered on an x-y recorder.

The Pyrex fluorescence cell was semicylindrical

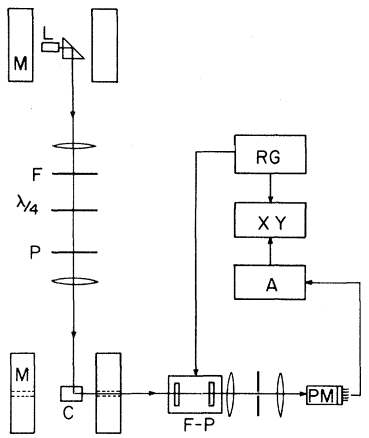

FIG. 1. Arrangement of the apparatus. L, exciting light source; F, interference filter; P, polaroid; C, fluorescence cell; M, electromagnets; F-P, interferometer; A, electrometer amplifier and RG, ramp generator, both connected to X-Y plotter.

in shape, 6 cm long and 2.5 cm in diameter. It was equipped with a side arm, 4 cm long and 1.5 cm in diameter, which contained an excess of metallic potassium, and with two plane windows at right angles to each other located at the front end. The cell was mounted in an oven consisting of two compartments: one containing the body of the cell in which a constant temperature was maintained using noninductively wound heaters, and the other containing the side-arm in which a precisely controlled temperature in the range 344–387 K was produced by a copper coil through which silicone oil was circulated from an ultrathermostat. Temperatures were measured using several copper-constantan thermocouples attached at various points on the fluorescence cell and side-arm. In order to prevent condensation on the cell windows, the main oven was always kept at about 35 K above the temperature of the side-arm. The cell was connected by a capillary folded inside the oven to a vacuum and gas-filling system.

The fluorescence was excited in the rectangular corner between the semicircular entrance and rectangular observation windows so that the fluorescent light traversed a distance of about 3 mm in the vapor before emerging from the cell. It was then collimated and made incident on a piezoelectrically scanned Fabry-Perot interferometer (Burleigh model RC 140), fitted with mirrors of flatness $\lambda/200$ and 96% reflectance in the range 7400–9200 Å, spaced 0.34 cm apart, providing an effective instrumental finesse of 30 and a free spectral range of 1.47 cm^{-1}. The light leaving the interferometer was focused at a 0.5-mm pinhole, whose size was determined so as not to detract from the overall finesse.[17] The fluorescent spectrum produced by scans of the interferometer was focused onto the photocathode of an ITT FW 118 photomultiplier, whose output signal amplified with a high-speed current amplifier (Keithley model 427), was applied to the y axis input of an x-y plotter to whose x axis was applied a fraction of the ramp voltage used to activate the piezoelectric element of the interferometer. At the beginning of each experimental run, the temperature of the cell and side-arm was lowered to "freeze out" the potassium vapor and determine the level of stray scattered light, which amounted to less than 0.2% of the direct fluorescence.

With the correct adjustment of the two magnetic fields to produce a coincidence between Zeeman components in the exciting light and in the absorbing vapor, excitation with σ^--polarized 7665-Å or 7699-Å radiation resulted in the selective population of the $4^2P_{3/2,-3/2}$ state[4] or the $4^2P_{1/2,-1/2}$ state,[3] respectively. At low vapor densities and in the absence of a buffer gas, the observed fluorescence would be expected to consist of just one component arising from the decay of the optically populated Zeeman substate. However, because of imperfection of the circular polarizer, the exciting light contained a small σ^+ admixture, which caused the excitation of the $^2P_{3/2,3/2}$ (or $^2P_{1/2,1/2}$) state. This "σ^+ leak," which was accurately determined, amounted to about 2% of the incident intensity and required appropriate corrections to spectral intensity measurements.

An increase in the potassium vapor density or the addition of a buffer gas caused the appearance of collisionally induced Zeeman components in the fluorescent spectrum, whose intensities depended on the density of the ground-state atoms acting as collision partners. A typical $^2P_{3/2}$ Zeeman spectrum

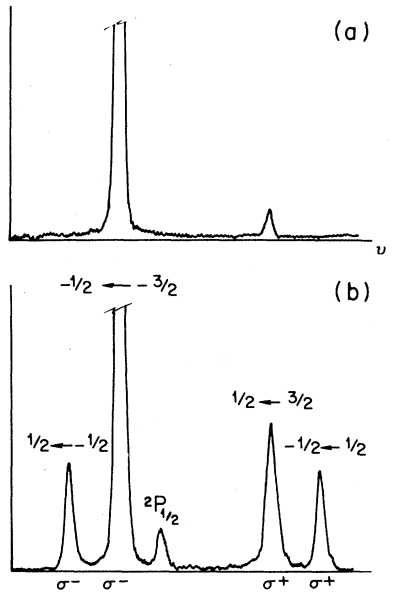

FIG. 2. Fluorescent spectrum produced by an interference scan of $\sigma^{\pm}$-polarized radiation emitted in the decays $4^2S_{1/2,\pm 1/2} \leftarrow 4^2P_{3/2,m}$ with the upper and lower Zeeman substates indicated. (a) In pure K vapor density 5×10^9 cm^{-3} the spectrum consists of one component arising from the optically populated $^2P_{3/2,-3/2}$ state; the faint $^2P_{3/2,3/2}$ component is due to σ^+ leakage through the polarizer. (b) Addition of 1-Torr Ar produces transfers to and emission from the other Zeeman substates. The $(-\frac{1}{2} \leftarrow -\frac{3}{2})$ and $(\frac{1}{2} \leftarrow \frac{3}{2})$ peak heights measured in this trace were in the ratio 4:1. The spectrum includes a $^2P_{1/2}$ component due to $^2P_{3/2} \rightarrow {}^2P_{1/2}$ transfer; the second component is located in the shoulder of the $\frac{1}{2} \leftarrow \frac{3}{2}$ peak.

produced by K-Ar collisions is shown in Fig. 2; the peak separations were measured by calibrating the system using the known hyperfine structure of the 8943.46-Å Cs line.[18] The intensity measurements were carried out in three experimental runs with argon (at constant K densities) and five with pure potassium vapor, each run covering the full pressure range of the experiment. At each Ar or K density ten scans of the spectrum were recorded, each consisting of two interference orders. The scatter between intensities measured at identical temperatures and pressures did not exceed 10%. The experiments with Ar were carried out at side-arm temperatures of 348 K (corresponding to 6.3×10^{10} K atoms/cm^3) and 356 K (1.3×10^{11} K atoms/cm^3) for the $^2P_{3/2}$ state, and at 344 K (4.8×10^{10} K atoms/cm^3) for the $^2P_{1/2}$ state. In the experiments with pure potassium, the side-arm temperatures ranged from 368 to 387 K, corresponding to a density range $(3-12)\times10^{11}$atoms/cm^3. The potassium densities were calculated from temperature-vapor pressure relations.[19]

In order to calculate the cross sections from the experimental data, account had to be taken of radiation trapping, which causes the effective lifetime of the resonance 4^2P state to exceed its "natural" lifetime. Among the various methods[20] that could be used to make corrections for imprisonment of radiation, Milne's radiation diffusion theory[21] appeared most suitable at the potassium densities and optical depths that were used in the experiments. The theory permits the calculation of the effective lifetime τ in terms of the "natural" lifetime τ_0,

$$(\tau/\tau_0)=1+(k_0l/\beta)^2\ , \tag{22}$$

where β is the first root of the equation

$$\tan\beta=k_0l/\beta\quad(0\leq\beta\leq\pi/2)\ . \tag{23}$$

The opacity k_0l was evaluated at each potassium density with $l=3$ mm and k_0 calculated assuming a Doppler shape of the spectral lines which is justified at the very low pressures.[6] Because of the Zeeman splitting, all optical depths must be multiplied by a factor $\frac{17}{40}$ for the $^2P_{3/2}$ level and by $\frac{3}{5}$ for the $^2P_{1/2}$ level.[22] The resulting lifetime τ exceeded τ_0 by about 27–50% in the K-Ar mixtures. The correctness of these corrections was indicated by the fact that identical results (within stated limits of error) were obtained from measurements performed at different potassium densities. In pure potassium vapor where higher densities were employed to obtain an acceptable signal-to-noise ratio, the effective lifetime varied with the density and, at the highest density 12×10^{11} cm^{-3}, $\tau=12\tau_0$.

IV. RESULTS AND DISCUSSION

The measured (and corrected) intensities of the Zeeman components in the fluorescent spectra are plotted in Figs. 3–5 relative to the intensities of the components emitted in the decay of the optically populated $^2P_{1/2,-1/2}$ or $^2P_{3/2,-3/2}$ Zeeman substates against the densities of the ground-state K or Ar atoms. Since it was intended that the intensities be representative of the Zeeman populations, the intensities $I_{1/2}$ and $I_{-1/2}$ in the $^2P_{3/2}$ spectrum were multiplied by a factor of 3. To eliminate effects due to radiation trapping, which is density dependent, the intensity ratios plotted for pure K vapor in Figs. 3 and 5 were divided by τ, the effective lifetime which was calculated at each potassium density. The linearity of these plots and the fact that they pass through the origin suggest good consistency of the applied corrections for radiation trapping. The plots are expected to be linear at low densities at which the collision frequencies are very low, amounting to less than one collision per lifetime of the 4^2P state. Under these conditions only one collisional transfer is likely to occur from the optically populated to another Zeeman substate. At densities above 5×10^{15} cm^{-3}, subsequent transfers (including back transfer) manifest themselves by a curva-

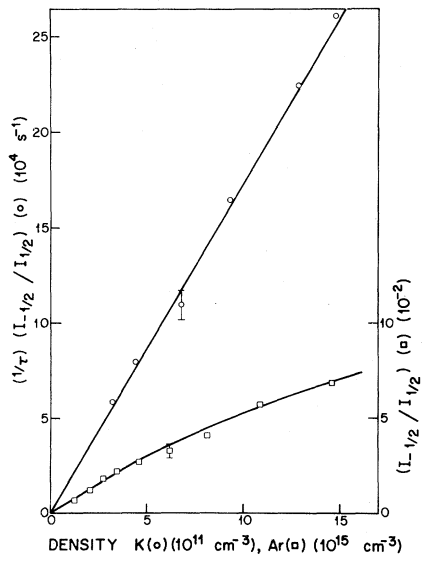

FIG. 3. Plots of Zeeman fluorescent intensity ratios for the $4^2P_{1/2}$ state. ○, results from pure K vapor (in units of 10^4 s^{-1}); □, effects of K-Ar collisions (in units of 10^{-2}). The solid curves represent least-squares fits to the data points. The error bars show statistical scatter of the measurements and are representative of each system.

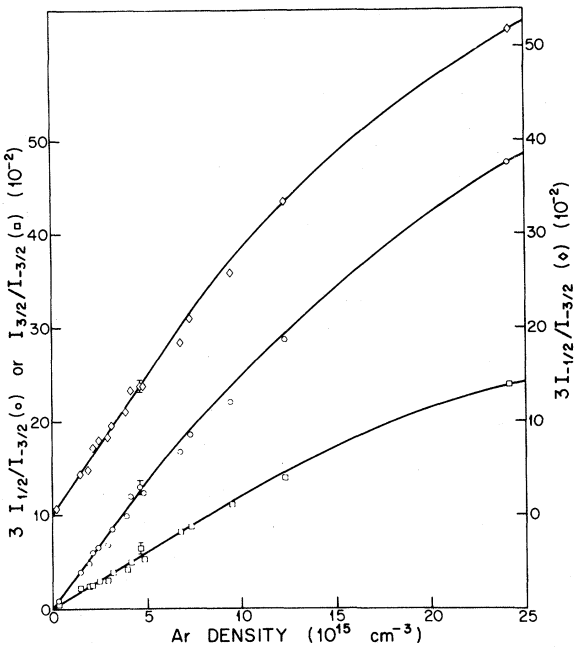

FIG. 4. Plots of Zeeman fluorescent intensity ratios (in units of 10^{-2}) for the $4^2P_{3/2}$ state showing effects of m_J mixing induced in K-Ar collisions. The solid curves represent least-squares fits to the data points. The error bars represent statistical scatter of the measurements.

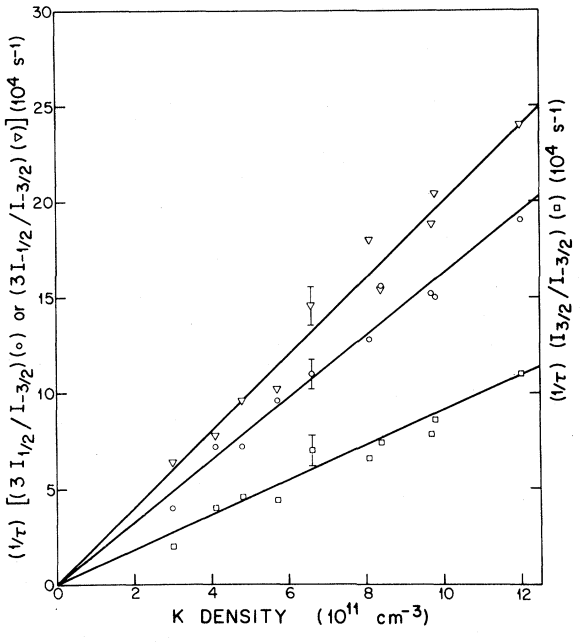

FIG. 5. Plots of Zeeman fluorescent intensity ratios (in units of $10^4 s^{-1}$) for the $4^2P_{3/2}$ state showing effects of m_J mixing induced by K-K collisions. The solid lines represent least-squares fits to the data points. The error bars represent statistical scatter of the measurements.

ture in the K-Ar plots. Under single-collision conditions, the rate equations (3) may be simplified to yield the following expressions for the transfer cross sections:

$$Q_J(m\rightarrow m')=(1/Nv_r\tau)N_{m'}/N_m\ . \tag{24}$$

Equation (24) permits the calculation of the cross sections $Q(m\rightarrow m')$ from the K-K plots and the linear parts of the K-Ar plots in Figs. 3—5, except for $Q_{3/2}(\frac{1}{2}\leftrightarrow-\frac{1}{2})$. It was found that the values thus obtained agreed to within 5% with the cross sections calculated from all the data using Eqs. (13), (14), and (16)—(19), bearing in mind that, under our conditions of geometry and polarization, for the $^2P_{1/2}$ state,

$$s^{(1)}_{1/2}/s^{(0)}_{1/2}=1\ , \tag{25}$$

and for the $^2P_{3/2}$ state,

$$s^{(1)}_{3/2}/s^{(0)}_{3/2}=\frac{3}{\sqrt{5}},\quad s^{(2)}_{1/2}/s^{(0)}_{1/2}=1\ ,$$
$$s^{(3)}_{3/2}/s^{(0)}_{3/2}=\frac{1}{\sqrt{5}}\ , \tag{26}$$

where the $s^{(L)}_J$ multipole components are obtained by an expansion of S_m analogous to that of N_m carried out in Eqs. (5)—(10). The resulting relaxation cross sections $\Lambda^{(1)}_J$, $\Lambda^{(2)}_J$, and $\Lambda^{(3)}_J$, upon substitution in Eqs. (15)—(19), gave the $Q_J(m\rightarrow m')$ Zeeman mixing cross sections. Finally, the relaxation cross sections $\Lambda^{(L)}_J$ were combined in Eq. (21) with $\sigma^{(0)}_J$, the $^2P_{1/2}-{}^2P_{3/2}$ fine-structure mixing cross sections to produce $\sigma^{(L)}_J$, the cross sections for multipole decay. In the case of K-K collisions $\sigma^{(0)}_J\ll\Lambda^{(L)}_J$ and $\sigma^{(L)}_J\equiv\Lambda^{(L)}_J$. For the K-Ar system, recently remeasured values[23] $\sigma^{(0)}_J$ were used. All the cross sections, which are listed in Tables I and II, are estimated to be accurate within $\pm15\%$ or better with the uncertainty arising from scatter in intensity measurements and from the possible systematic error in the K and Ar densities. As expected,[24] the cross sections for resonant K-K collisions exceed by over 2 orders of magnitude the K-Ar cross sections. The K-K cross sections are significantly smaller than the values $\sigma^{(1)}_{1/2}$, $\sigma^{(1)}_{3/2}$, and $\sigma^{(2)}_{3/2}$ reported previously,[5,6] which were inflated because of the σ^+ light leak through the circular polarizer, which was discovered and for which corrections were made in the present experiment. There is adequate agreement with the theoretical values calculated by Carrington *et al.*[11] though the relative sizes of their

TABLE I. Cross sections for K-K collisions (in 10^{-12} cm^2).

Designation	This investigation	Carrington *et al.*[11] (theory)	Other results
$\Lambda^{(1)}_{1/2}$ or $\sigma^{(1)}_{1/2}$	5.7±0.9	4.9	40[a]
$\Lambda^{(1)}_{3/2}$ or $\sigma^{(1)}_{3/2}$	8.1±1.4	6.2	17[b]
$\Lambda^{(2)}_{3/2}$ or $\sigma^{(2)}_{3/2}$	11.4±2.0	5.6	21[b]
$\Lambda^{(3)}_{3/2}$ or $\sigma^{(3)}_{3/2}$	9.8±1.5	6.1	
$Q_{1/2}(-\frac{1}{2}\leftrightarrow\frac{1}{2})$	2.8±0.5	2.4[c]	
$Q_{3/2}(-\frac{1}{2}\leftrightarrow\frac{1}{2})$	2.0±0.8	1.7[c]	
$Q_{3/2}(-\frac{3}{2}\leftrightarrow-\frac{1}{2})$	3.1±0.6	1.4[c]	
$Q_{3/2}(-\frac{3}{2}\leftrightarrow\frac{1}{2})$	2.6±0.5	1.4[c]	
$Q_{3/2}(-\frac{3}{2}\leftrightarrow\frac{3}{2})$	1.3±0.4	1.7[c]	0.8[d]

[a]Reference 5.
[b]Reference 6.
[c]Derived from Ref. 11 and Eqs. (15)–(19).
[d]Reference 8 for Na.

cross sections differ from those found here. There is also agreement within order of magnitude with Gay and Schneider's[8] $Q_{3/2}(-\frac{3}{2}\leftrightarrow\frac{3}{2})$ for Na.

As is apparent in Table II, depolarizing collisions with noble gases have been studied much more extensively than K-K collisions. For the $^2P_{1/2}$ state, the previously reported K-Ar cross section[3] was determined at K densities at which radiation trapping was significant, though no allowance for it was made. A recalculation using the corrected value of τ produces very good agreement with the present cross section $\Lambda^{(1)}_{1/2}$ which, as expected,[24,25] lies between the recently determined values[9] for Ne and Kr; a parallel relationship may be seen in the $^2P_{3/2}$ state with respect to $\Lambda^{(1)}_{3/2}$, $\Lambda^{(2)}_{3/2}$, and $\Lambda^{(3)}_{3/2}$, where there is excellent accord with previously measured disorientation and disalignment cross sections[4] and satisfactory agreement with $\sigma^{(L)}_{3/2}$, approximately calculated by Lewis, Wheeler, and Wilson[10] who also determined $\sigma^{(1)}_{3/2}$ using the Hanle effect and correcting their measurements for the effects of nuclear spin. The agreement is not nearly as good for

TABLE II. Cross sections for K-Ar collisions (in 10^{-16} cm^2).

Designation	This investigation	Berdowski *et al.*[3,4] corrected for τ	Lewis *et al.*[10]	Boggy and Franz[9] Ne	Boggy and Franz[9] Kr
$\Lambda^{(1)}_{1/2}$	65 ±10	73		56	81
$Q_{1/2}(-\frac{1}{2}\leftrightarrow\frac{1}{2})$	32 ± 5	36			
$\sigma^{(0)}_{1/2}$	16[a]				
$\sigma^{(1)}_{1/2}$	81 ±12		278[b]; 35[c]		
$\Lambda^{(1)}_{3/2}$	175 ±25	164		103	270
$\Lambda^{(2)}_{3/2}$	230 ±35	240		146	341
$\Lambda^{(3)}_{3/2}$	190 ±30			111	276
$Q_{3/2}(-\frac{1}{2}\leftrightarrow\frac{1}{2})$	36.8±16.0			18.6[d]	52.5[d]
$Q_{3/2}(-\frac{3}{2}\leftrightarrow-\frac{1}{2})$	59.8± 3.0			37.7[d]	86.2[d]
$Q_{3/2}(-\frac{3}{2}\leftrightarrow\frac{1}{2})$	55.3± 2.0			35.3[d]	84.4[d]
$Q_{3/2}(-\frac{3}{2}\leftrightarrow\frac{3}{2})$	30.8± 2.0			15.4[d]	50[d]
$\sigma^{(0)}_{3/2}$	11.2[a]				
$\sigma^{(1)}_{3/2}$	186 ±27		242[b]; 187[c]		
$\sigma^{(2)}_{3/2}$	241 ±37		346[b]		
$\sigma^{(3)}_{3/2}$	201 ±32		225[b]		

[a]Reference 23.
[b]Approximate theory.
[c]From Hanle experiment.
[d]Derived from Ref. 9 and Eqs. (15)–(19).

TABLE III. Ratios of $\Lambda_{3/2}^{(L)}$ relaxation cross sections.

Designation	This investigation	Boggy and Franz[9] Ne	Boggy and Franz[9] Kr	Okunewich and Perel[26] (theory)	Lewis *et al.*[10] (theory, "case c")[a]
$\Lambda_{3/2}^{(1)}/\Lambda_{3/2}^{(2)}$	0.76	0.71	0.79	0.81	0.69
$\Lambda_{3/2}^{(2)}/\Lambda_{3/2}^{(3)}$	1.21	1.32	1.24	1.13	1.57
$\Lambda_{3/2}^{(1)}/\Lambda_{3/2}^{(3)}$	0.92	0.93	0.98	0.91	1.08

[a] $\Lambda_{3/2}^{(L)}$ were obtained by subtraction of $\sigma_{3/2}^{(0)}$ taken from Ref. 24, from authors' $\sigma_{3/2}^{(L)}$.

the $^2P_{1/2}$ case, where the calculated $\sigma_{1/2}^{(1)}$ cross section greatly exceeds all the experimental values. A worthwhile comparison can be made with the predictions of Okunewich and Perel[26] who calculated ratios of the $^2P_{3/2}$ relaxation cross sections assuming van der Waals interaction between the colliding atoms. Table III shows the predicted $\Lambda_{3/2}^{(L)}$ ratios, which are in total harmony with the corresponding ratios found in this investigation as well as those calculated from the values of Boggy and Franz for Ne and Kr.[9] The corresponding $\Lambda_{3/2}^{(L)}$ ratios were also derived from the theoretical $\sigma_{3/2}^{(L)}$ of Lewis *et al.*[10] by subtracting from them the experimentally determined[23] $\sigma_{3/2}^{(0)}$. The resulting agreement is not nearly as good as with the values of Okunewich and Perel, perhaps reflecting the approximate nature of the theoretical treatment.[10]

ACKNOWLEDGMENTS

The authors wish to express their appreciation to Professor Baylis for various helpful discussions, and to thank Professor Franz for permission to quote his results[9] before publication. This research was supported by the Natural Sciences and Engineering Research Council of Canada.

[1]W. E. Baylis, in *Progress in Atomic Spectroscopy, Part B* edited by W. Hanle and H. Kleinpoppen (Plenum, New York, 1979), and references therein.
[2]See, for example, R. B. Bulos and W. Happer, Phys. Rev. A 4, 849 (1971).
[3]W. Berdowski and L. Krause, Phys. Rev. 165, 158 (1968).
[4]W. Berdowski, T. Shiner, and L. Krause, Phys. Rev. A 4, 984 (1971).
[5]P. Skalinski and L. Krause, Can. J. Phys. 57, 2222 (1979).
[6]P. Skalinski and L. Krause, Can. J. Phys. 58, 1500 (1980).
[7]J.-C. Gay and W. B. Schneider, Z. Phys. A278, 211 (1976).
[8]J.-C. Gay and W. B. Schneider, Phys. Rev. A 20, 905 (1979).
[9]R. Boggy and F. A. Franz, Phys. Rev. A 25, 1887 (1982).
[10]E. L. Lewis, C. S. Wheeler, and A. D. Wilson, J. Phys. B 10, 2619 (1977).
[11]C. G. Carrington, D. N. Stacey, and J. Cooper, J. Phys. B 6, 417 (1973).
[12]G. Copley and L. Krause, Can. J. Phys. 47, 533 (1969).
[13]U. Fano, Rev. Mod. Phys. 29, 74 (1957).
[14]A. Omont, J. Phys. (Paris) 26, 26 (1965).
[15]P. Skalinski, Ph.D thesis, University of Windsor, 1982 (unpublished).
[16]W. Berdowski, T. Shiner, and L. Krause, Appl. Opt. 6, 1683 (1967).
[17]R. Chabbal, J. Rech. CNRS 24, 138 (1953).
[18]S. Millman and P. Kusch, Phys. Rev. 58, 438 (1940).
[19]A. N. Nesmeyanov, *Vapor Pressure of the Elements* (Academic, New York, 1963).
[20]R. P. Blickensderfer, W. H. Breckenridge, and J. Simons, J. Phys. Chem. 80, 653 (1976).
[21]E. A. Milne, J. London Math. Soc. 1, 40 (1926).
[22]W. E. Baylis (private communication). $\frac{17}{40}$ represents the average of $\frac{21}{40}$ for the $\sigma^+(\frac{3}{2}, \frac{3}{2} \rightarrow \frac{1}{2}, \frac{1}{2})$ component and $\frac{13}{40}$ for the $\sigma^+(\frac{3}{2}, \frac{1}{2} \rightarrow \frac{1}{2}, -\frac{1}{2})$ component. See also J. S. Deech and W. E. Baylis, Can. J. Phys. 49, 90 (1971).
[23]J. Ciurylo and L. Krause, J. Quant. Spectrosc. Radiat. Transfer (in press).
[24]L. Krause, in *The Excited State in Chemical Physics,* edited by J. W. McGowan (Wiley, New York, 1975).
[25]T. F. Gallagher, S. A. Edelstein, and R. M. Hill, Phys. Rev. A 15, 1945 (1977).
[26]A. I. Okunewich and V. I. Perel, Zh. Eksp. Teor. Fiz. 58, 666 (1970) [Sov. Phys.—JETP 31, 356 (1970)].